# α-Conotoxin RegIIa Targeting Nicotinic Acetylcholine Receptors: Mutagenesis Studies Improving Selectivity and Potency

**CONFERENCE PAPER** *in* BIOPHYSICAL JOURNAL · JANUARY 2013

Impact Factor: 3.97 · DOI: 10.1016/j.bpj.2012.11.3505



**4 AUTHORS**, INCLUDING:

Shiva Nag Komeplla

RMIT University

**14** PUBLICATIONS **76** CITATIONS

SEE PROFILE

Andrew Hung

RMIT University

**39** PUBLICATIONS **748** CITATIONS

SEE PROFILE

David J. Adams

University of Wollongong

**270** PUBLICATIONS **7,883** CITATIONS

SEE PROFILE

Biochemical Pharmacology 83 (2012) 419–426

Contents lists available at SciVerse ScienceDirect

Biochemical Pharmacology

journal homepage: www.elsevier.com/locate/biochempharm

# RegIIA: An α4/7-conotoxin from the venom of *Conus regius* that potently blocks α3β4 nAChRs

Aldo Franco [a], Shiva N. Kompella [b], Kalyana B. Akondi [c], Christian Melaun [d], Norelle L. Daly [c], Charles W. Luetje [e], Paul F. Alewood [c], David J. Craik [c], David J. Adams [b], Frank Marí [a,*]

[a] Department of Chemistry & Biochemistry, Florida Atlantic University, 777 Glades Rd., Boca Raton, FL 33431, USA
[b] Health Innovations Research Institute, RMIT University, Melbourne, VIC 3083, Australia
[c] Institute for Molecular Bioscience, The University of Queensland, Brisbane, QLD 4072, Australia
[d] Biodiversity and Climate Research Centre, Senckenberganlage 25, D-60325 Frankfurt am Main, Germany
[e] Department of Molecular & Cellular Pharmacology, Miller School of Medicine, University of Miami, Miami, FL 33101, USA

ARTICLE INFO

*Article history:*
Received 27 August 2011
Accepted 7 November 2011
Available online 16 November 2011

*Keywords:*
*Conus regius*
α-Conotoxin
Nicotinic acetylcholine receptor
NMR structure
Nicotine addiction

ABSTRACT

Neuronal nicotinic acetylcholine receptors (nAChRs) play pivotal roles in the central and peripheral nervous systems. They are implicated in disease states such as Parkinson's disease and schizophrenia, as well as addictive processes for nicotine and other drugs of abuse. Modulation of specific nAChRs is essential to understand their role in the CNS. α-Conotoxins, disulfide-constrained peptides isolated from the venom of cone snails, potently inhibit nAChRs. Their selectivity varies markedly depending upon the specific nAChR subtype/α-conotoxin pair under consideration. Thus, α-conotoxins are excellent probes to evaluate the functional roles of nAChRs subtypes.

We isolated an α4/7-conotoxin (RegIIA) from the venom of *Conus regius*. Its sequence was determined by Edman degradation and confirmed by sequencing the cDNA of the protein precursor. RegIIA was synthesized using solid phase methods and native and synthetic RegIIA were functionally tested using two-electrode voltage clamp recording on nAChRs expressed in *Xenopus laevis* oocytes. RegIIA is among the most potent antagonist of the α3β4 nAChRs found to date and is also active at α3β2 and α7 nAChRs. The 3D structure of RegIIA reveals the typical folding of most α4/7-conotoxins. Thus, while structurally related to other α4/7 conotoxins, RegIIA has an exquisite balance of shape, charge, and polarity exposed in its structure to potently block the α3β4 nAChRs.



## 1. Introduction

Neuronal nicotinic acetylcholine receptors (nAChRs) play an important role in the central and peripheral nervous system and are implicated in certain disease states including Parkinson's disease, schizophrenia, depression, Alzheimer's disease, and nicotine addiction [1]. These receptors are nicotine-sensitive ligand gated ion channels that are endogenously activated by acetylcholine. Structurally, most neuronal nAChRs are hetero-pentamers of α2-6 and β2-4 subunits combined in different stoichiometries [2]. There are homomeric nAChRs, notable among these is the α7 nAChR, and heteromeric receptors that are composed of only alpha subunits such as α9α10 nAChRs.

The specific combinations of α and β subunits mediate the diverse population of neuronal nAChRs subtypes with different subtypes having a specific function and distribution in the central and peripheral nervous system. α4β2 nAChRs are the predominant subtype in the brain, they have the highest affinity for nicotine ($K_i$ = 0.6–10 nM) and account for >90% of binding of nicotine in brain tissues [3]. Transgenic knockout of α4 or β2 subunits eliminate nicotine self-administration in mice. Re-instatement of these subunits in the knockout restores nicotine self-administration, implicating this receptor in nicotine addiction [4].

Other nAChR subtypes, particularly the α3β4, can also be involved in addiction of nicotine and other drugs of abuse [4]. The α3β4 is the predominant nAChR in the sensory and autonomic ganglia and in subpopulations of CNS neurons, such as medial habenula and dorsal medulla [2]. This receptor is involved in the mesolimbic dopamine pathway and is thought to be important in certain feedback rewarding effects under a substance abuse

*Abbreviations:* AChBP, acetylcholine-binding protein; CNS, central nervous system; DMSO, dimethyl sulfoxide; DTT, dithiothreitol; EST, expressed sequence tag; $GABA_BR$, γ-aminobutyric acid type B receptor; IAM, iodoacetamide; nAChR, nicotinic acetylcholine receptor; PCR, polymerase chain reaction; RACE, rapid amplification of cDNA ends; SCUBA, self-contained underwater breathing apparatus; SE-HPLC, size exclusion HPLC; SPPS, solid phase peptide synthesis; TFA, trifluoroacetic acid.

* Corresponding author. Tel.: +1 561 2973315; fax: +1 561 2972759.
*E-mail address:* mari@fau.edu (F. Marí).

0006-2952/$ – see front matter © 2011 Published by Elsevier Inc.
doi:10.1016/j.bcp.2011.11.006

regimen. Furthermore, nicotine-induced hypolocomotion is reduced in β4 null mice, thus emphasizing the importance of α3β4 in the nicotine related effects in the CNS [5]. While the involvement of α3β4 receptors in psychostimulant and drug-abusive behavior has been established [6], the lack of adequate molecular probes that allow exploring the neurophysiology of these receptors is a limiting factor for establishing their precise role in addiction.

α-Conotoxins, ubiquitous compounds found in the venoms of cone snails [7], are short disulfide-constrained peptides that target various nAChR subtypes. α-Conotoxin sequences have four cysteines arranged in CC–$X_n$–C–$Y_m$–C pattern, where $X_n$ is a loop of amino acids with $n$ = 3–4 and $Y_m$ is a loop of amino acids with $m$ = 3–7. The sizes of the loops are used for α-conotoxin classification (i.e., an α4/7-conotoxin has 4 residues in the X loop and 7 residues in the Y loop). The number and nature of the amino acids in these loops are defining for the binding and selectivity of α-conotoxins towards nAChRs subtypes. The sequences of α-conotoxins are species-specific, therefore, the discovery of new α-conotoxins can provide new tools for the functional exploration of nAChR subtypes. In general, α-conotoxins target more than one nAChR subtype; however, their selectivity and potency can vary widely. Here we describe the discovery, together with the biochemical, biophysical and functional characterization of RegIIA, an α4/7-conotoxin isolated from the venom of *Conus regius*, a worm-hunting cone snail species that inhabits the Western Atlantic Ocean. RegIIA is among the most potent antagonist of α3β4 nAChRs to date, and it does not inhibit the α4β2 subtype. This selectivity profile makes RegIIA a prospective probe for studying nicotine addiction processes. RegIIA has a classical α-conotoxin globular structure (ω-shaped fold) indicating that it has an exquisite balance of shape, charges, and polarity exposed on its surface to enable it to potently block the α3β4 nAChR.

## 2. Methods and materials

### 2.1. Specimen collection, RegIIA isolation and characterization

Specimens of *C. regius* (35–70 mm in length) were collected off the Florida Keys (Plantation Key), USA, using SCUBA at depths ranging from 2 to 10 m. Venom ducts dissected from specimens of *C. regius* were homogenized in 0.1% TFA (Fisher Scientific, PA) at 4 °C. Whole extracts were centrifuged at 10,000 × *g* for 20 min, at 4 °C, and the resulting pellets were washed three times with 0.1% TFA and re-centrifuged under identical conditions. The supernatants containing the soluble peptides were pooled, lyophilized, and stored at −80 °C until further use. Batches of 50 mg of crude venom were separated by SE-HPLC on a Pharmacia Superdex-30 column (2.5 cm × 100 cm) equilibrated and eluted with 0.1 M $NH_4HCO_3$ (Fisher Scientific, PA). Further separation of fractions obtained from the Superdex-30 column was performed on a Superdex Peptide (Amersham Biosciences, MA) column (10 mm × 300 mm) equilibrated and eluted with 0.1 M $NH_4HCO_3$. Chromatographic fractions were monitored at λ = 220, 250, and 280 nm. Additional purification of peptide-containing peaks was achieved by RP-HPLC on a C18 semipreparative column (Vydac, 218TP510, 10 mm × 250 mm; 5 μm particle diameter; 300 Å pore size). Further peptide purification was carried out by re-chromatographing fractions on an analytical C18 column (Vydac, 238TP54, 4.6 mm × 250 mm; 5 μm particle diameter; 300 Å pore size). For semipreparative and analytical RP-HPLC separation, the buffers were 0.1% TFA (buffer A) and 0.1% TFA in 60% acetonitrile (Fisher Scientific, PA) (buffer B). Peptides were eluted with an incremental linear gradient of 1% B/min. All HPLC fractions were manually collected, lyophilized and kept at −40 °C prior to further use.

Reduction and alkylation of cystine groups were carried out as previously described [8] with slight modifications. An aliquot of each peptide (~1 pmol) was dried, re-dissolved in 0.1 M Tris–HCl (Fisher Scientific, PA) (pH 8.2), 5 mM EDTA (Fisher Scientific, PA), 0.1% sodium azide and reduced with 6 mM DTT (Fisher Scientific, PA). Following incubation at 60 °C for 30 min, peptides were alkylated in a final volume of 15 μl with 20 mM IAM (Sigma–Aldrich, MO) and 2 μl of $NH_4OH$ (Fisher Scientific, PA) (pH 10.5) at room temperature for 1 h in the dark. The reduced and alkylated peptides were purified using a Zip Tip (C18, size P10, Millipore, MA). Alkylated peptides were adsorbed onto Biobrene-treated glass fiber filters and amino acid sequencing was carried out by Edman degradation using an Applied Biosystems Procise model 491A Sequencer. Positive ion MALDI-TOF mass spectrometry was carried out on an Applied Biosystems Voyager-DE STR spectrometer. Samples were dissolved in 0.1% TFA, 50% acetonitrile, and applied on α-cyano-4-hydroxycinnamic acid matrix. Amidation of the C-terminus was determined by the difference between the calculated and experimental molecular weight and confirmed by nanoNMR spectroscopy.

### 2.2. Cloning and sequencing of the precursor of RegIIA

One venom duct from *C. regius* was removed from the freshly sacrificed animal on dry ice and stored at −70 °C. Approximately 1 cm of the duct was used for mRNA isolation with the Dynabeads® mRNA DIRECT™ Kit (Invitrogen, CA). First strand cDNA synthesis was performed as described previously [9]. 3′-RACE PCR was performed using a 5′ forward primer (5′-ATG GGC ATG CGG ATG ATG TTC-3′) binding on the conserved signal sequence of the A-superfamily [10], the reverse primer was a shorter version of the adapter primer without the poly dT tail as reverse primer. The PCR conditions consisted of an initial denaturation of 94 °C for 2 min followed by 40 cycles of 94 °C for 1 min, 55 °C for 1 min, and 72 °C for 1 min. 3′-RACE PCR products were ligated into the T-tailed plasmid vector pGEM®-T Easy (Promega, WI). The ligation products were transformed into NEB 5-alpha competent *E. coli*. Transformed colonies were screened using blue white selection. Plasmid DNA of 20 clones, containing an insert of the expected size, was isolated using the QIAprep Spin Miniprep kit (Qiagen, MD) and both strands of the insert were sequenced. Nucleotide sequences were analyzed using Bioedit and MEGA 4 [11]. The cDNA sequence of the here described conotoxin precursor has been deposited in the DDBJ/EMBL/GenBank Nucleotide Sequence Database under the accession number FR871900.

### 2.3. Peptide synthesis

The peptide was assembled by manual Boc-SPPS using HBTU-mediated (Buch, Switzerland) *in situ* neutralization protocol with *N*,*N*′-dimethylformamide (Auspep, Melbourne, Australia) as solvent [12]. HF (Matheson, TX) deprotection and cleavage was performed by treatment of the dried peptide resin (300 mg) with 10 mL HF/*p*-cresol/*p*-thio-cresol (Aldrich-Sigma, MO)(10:0.5:0.5, v/v/v) for 2 h at 0 °C. Following evaporation of the HF, the peptide was precipitated and washed with cold ether, filtered, and re-dissolved in 30 mL of 50% ACN/0.05% TFA and lyophilized. Oxidative folding was carried out in 0.1 M $NH_4HCO_3$ (pH 8.2, $c$ = 0.1 μM) resulting in formation of the globular isomer of RegIIA. The oxidation was monitored by RP-HPLC, LC–MS and MS, and the peptide isomers were isolated using preparative C18 RP-HPLC.

### 2.4. Electrophysiological recordings from exogenously expressed nAChRs in Xenopus oocytes

RNA preparation, oocyte preparation, and expression of nAChR subunits in *Xenopus* oocytes were performed as described

previously [13]. Briefly, plasmids with cDNA encoding the rat α3, α4, α10, β2, β4, α1, β1, γ, δ nAChR and human α7, α9 subunits cloned into the oocyte expression vector pNKS2 were used for mRNA preparation using mMESSAGE mMACHINE Kit (Ambion Inc., USA). All oocytes were injected with 5 ng of cRNA, and then kept at 18 °C in ND96 buffer (96 mM NaCl, 2 mM KCl, 1 mM $CaCl_2$, 1 mM $MgCl_2$, and 5 mM HEPES, at pH 7.4) supplemented with 50 μg/liter gentamycin (Sigma–Aldrich, MO) and 5 mM pyruvic acid (Sigma–Aldrich, MO) 2–5 days before recording. Membrane currents were recorded from *Xenopus* oocytes using either a standard electrophysiology voltage clamp setup [14] for native RegIIA or an automated workstation with eight channels in parallel for synthetic RegIIA, which included a compound delivery system with on-line analysis (OpusXpress™ 6000A workstation, Molecular Devices, Sunnyvale, CA) and a GeneClamp 500B amplifier (Molecular Devices) used in single channel voltage-clamp setup. The voltage-recording and current-injecting electrodes were pulled from borosilicate glass (GC150T-15, Harvard Apparatus Ltd.) and had resistances of 0.3–1.5 MΩ when filled with 3 M KCl. All recordings were conducted at room temperature (20–23 °C) using a bath solution of ND96 as described above. During recordings, the oocytes were perfused continuously at a rate of 1.5 ml/min, with 300 s incubation time for the conotoxin. Acetylcholine (Sigma–Aldrich, MO) (200 μM for α7, 30 μM for all other nAChR subtypes) was applied for 2 s at 5 ml/min, with 360 s washout periods between applications. Cells were voltage-clamped at a holding potential of −80 mV. Data were sampled at 500 Hz and filtered at 5 Hz. Peak current amplitude was measured before and following incubation of the toxin peptide [15]. Concentration–response curves for antagonists were fitted by unweighted nonlinear regression to the logistic equation

$$E_x = \frac{E_{max} X^{nH}}{X^{nH} + IC_{50}^{nH}}$$

where $E_x$ is the response, $X$ is the antagonist concentration, $E_{max}$ is the maximal response, $n$H is the slope factor, and $IC_{50}$ is the concentration of antagonist that gives 50% inhibition of the agonist response. All electrophysiological data were pooled ($n$ = 4–8 for each data point) and represent arithmetic means ± standard error of the fit. The data was processed using SigmaPlot 11.0 (Systat Software, Point Richmond, CA).

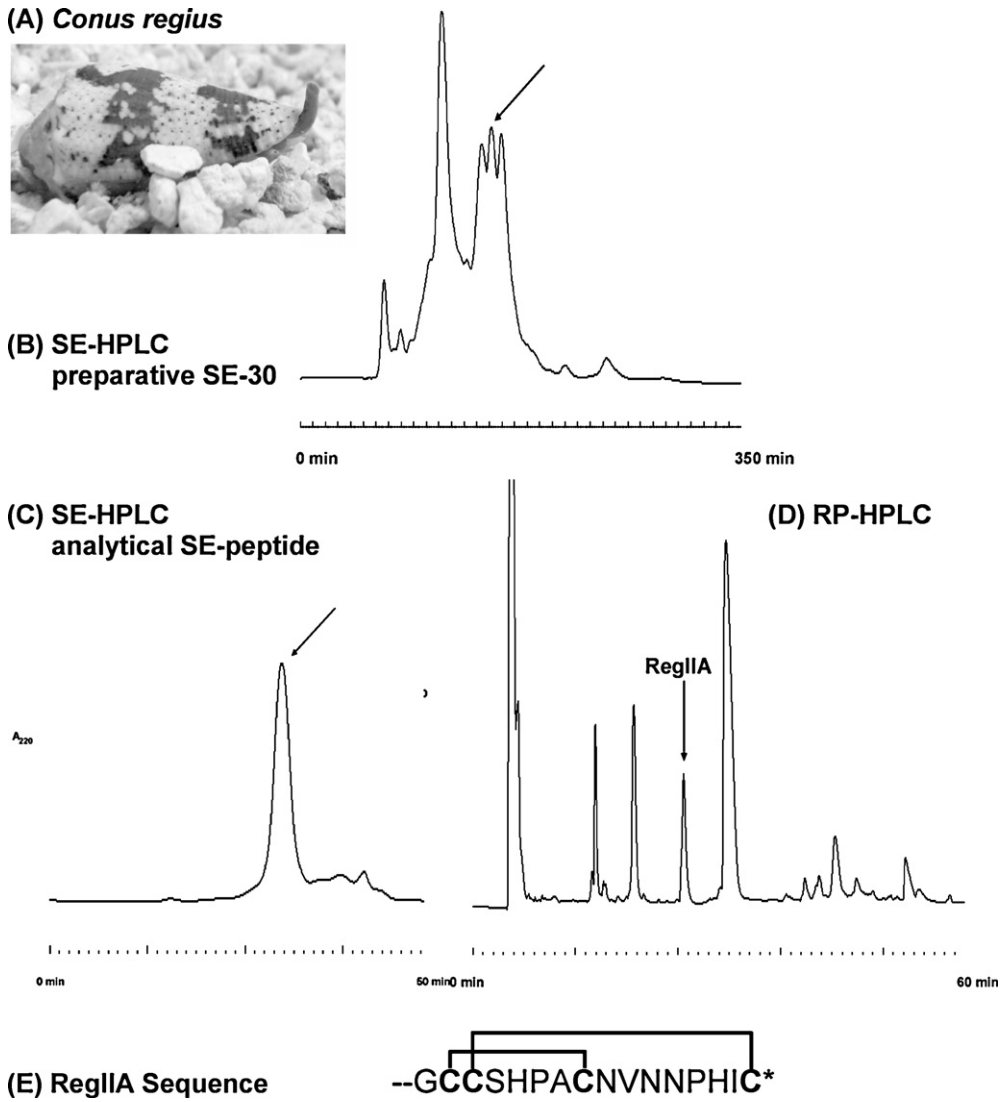


**Fig. 1.** Isolation of RegIIA from the venom of *C. regius*. (A) Live specimen of *C. regius*. (B) Venom separation by SE HPLC (Superdex 30) showing the absorbance profile at λ = 220 nm. The fraction containing RegIIA is indicated with an arrow and it was further purified using analytical SE HPLC (Superdex Peptide) (C). (D) UV trace of the analytical RP-HPLC separation. The RegIIA fraction is labeled with an arrow. (E) Amino acid sequence of RegIIA obtained by Edman degradation.

### 2.5. NMR spectroscopy and structure determination of RegIIA

NMR spectra of native RegIIA were acquired on a Varian Inova 500 MHz instrument as previously described [16]. Spectra of the native conotoxin were recorded at pH 3.60 and recorded at different temperatures (0, 10 and 25 °C). Spectra of synthetic RegIIA were recorded at 600 MHz (Bruker Avance NMR spectrometer) on a 0.5 mM solution of RegIIA in 10% $D_2O$/90% $H_2O$. The two-dimensional spectra were recorded and three-dimensional structures calculated as previously described [17]. Distance restraints were obtained from a NOESY spectrum recorded with a 200 ms mixing time at 17 °C.

## 3. Results

### 3.1. Discovery, characterization and synthesis of RegIIA

Fractionation of the venom of *C. regius* (SE and RP-HPLC) produced a pure peptide with a monoisotopic molecular mass of 1664.9 Da (Fig. 1). The amino acid sequence of the peptide (RegIIA) was obtained by Edman degradation (Fig. 1, Table 1), and corresponds to a 16-residue/2-disulfide bond hydrophilic conopeptide without aromatic residues, which has a sequence homology to other α4/7-conotoxins (Table 1). RegIIA was synthesized with all L-amino acids. NMR comparison of the native material with the synthetic one confirmed the identity of RegIIA, including its amidated C-terminus.

### 3.2. Cloning and sequence analysis of the cDNA of the precursor of RegIIA

The cDNA sequence precursor of RegIIA is shown in Table 2. This precursor encodes 65 amino acids and has a 22-residue signal sequence. A sequence similarity search [18] detected homologies with the precursors of A-superfamily of conotoxins [19] (Table 2). As found in the isolated peptide, the precursor of RegIIA predicts the mature peptide to be C-terminally amidated, since Gly is present at the loci preceding the C-terminal cleavage site [20].

### 3.3. Selective inhibition of α-conotoxin RegIIA of recombinant nAChR subtypes

The selectivity of RegIIA was examined by the inhibition of ACh-evoked currents mediated by various nAChRs subtypes expressed in *Xenopus* oocytes. ACh was applied at an interval of 5 min and the corresponding membrane currents were assessed. The peptide was applied to the bath 5 min prior to co-application of ACh plus peptide. Since RegIIA is homologous to several α3β2 blocking conotoxins, we initially used native RegIIA against that nAChR subtype (Fig. 2A) resulting in >80% inhibition with a 100 nM solution of the native peptide. The limited amounts of peptide isolated precluded a selectivity profile of nAChR subtypes. Synthetic RegIIA (1 μM) exhibited complete inhibition of ACh-evoked current amplitude produced by α3β4, α3β2, and α7 nAChRs. However, RegIIA did not inhibit either muscle (αβγδ) or α4β2 nAChRs ($n = 4–5$) (Fig. 3). RegIIA (1 μM) inhibited only $20 \pm 5\%$ of ACh-evoked current amplitude of α9α10 nAChR. Concentration–response curves of RegIIA display the order of selectivity and their corresponding $IC_{50}$ values for α3β2 ($33 \pm 4$ nM) > α3β4 ($97 \pm 20$ nM) > α7 ($103 \pm 23$ nM) (Fig. 3 and Table 3).

### 3.4. NMR spectroscopy of native and synthetic RegIIA

We were able to obtain $^1$H NMR (1D and 2D-TOCSY) of nanomolar quantities (nanoNMR) of the RegIIA conotoxin directly isolated from the venom of the cone snails. Comparison of the 2D-TOCSY spectra of native RegIIA with its synthetic counterpart, confirmed the proper synthesis and folding of synthetic material. The 2D NOESY of synthetic RegIIA showed spectral quality suitable for structural determination. $^1$H resonance assignments of RegIIA were achieved with the combined use of the TOCSY and NOESY spectra following the procedure outlined by Wuthrich [21]. Several unique spin systems within the sequence of RegIIA, Ser-4, Ala-7,

**Table 1**
Sequences of α-conotoxins related to RegIIA.

| α–conotoxin | Sequence | Species | Prey | Target⊥ | Ref |
|---|---|---|---|---|---|
| **RegIIA** | G**CC**SHPA**C**NVNNPHI**C*** | ***C. regius*** | (v) | nAChRs | |
| OmIA | G**CC**SHPA**C**NVNNPHI**C**G* | *C. omaria* | (m) | nAChRs, AChBP | [28] |
| GIC | G**CC**SHPA**C**AGNNQHI**C*** | *C. geographus* | (p) | nAChRs | [29] |
| Mr1.1 | G**CC**SHPA**C**SVNNPDI**C*** | *C. marmoreus* | (m) | nAChRs | [31] |
| PeIA | G**CC**SHPA**C**SVNHPEL**C*** | *C. pergrandis* | (ND) | nAChRs, $GABA_BR$ | [45] |
| AnIB | GG**CC**SHPA**C**AANNQDŶ**C*** | *C. anemone* | (v) | nAChRs | [32] |
| GID | IRDγ**CC**SNPA**C**RVNNOHV**C** | *C. geographus* | (p) | nAChRs | [30] |
| MII | G**CC**SNPV**C**HLEHSNL**C*** | *C. magus* | (p) | nAChRs | [14] |
| PIA | RDP**CC**SNPV**C**TVHNPQI**C*** | *C. purpurascens* | (p) | nAChRs | [41] |
| Vc1.1 | G**CC**SDPR**C**NYDHPEI**C*** | *C. victoriae* | (m) | nAChRs, $GABA_BR$ | [45] |
| EpI | G**CC**SDPR**C**NMNNPDŶ**C*** | *C. episcopatus* | (m) | nAChRs | [33] |
| AuIB | G**CC**SYPP**C**FATNPD–**C*** | *C. aulicus* | (m) | $GABA_BR$ | [39] |
| PnIA | G**CC**SLPP**C**AANNPDY**C*** | *C. pennaceus* | (m) | nAChRs, AChBP | [34] |

Amino acid conservations are denoted by light grey shade. Dark grey shaded amino acids are homologous within that loci of the set. The framework I scaffold formed by disulfide bonded cysteins are bold faced and boxed. ⊥ Target criteria: $IC_{50}$ or $K_i < 100$ nM. See Table 3 for selectivity towards nAChRs subtypes. γ, γ-carboxyglutamate; O, 4-hydroxyproline; Ŷ, sulfotyrosine; *, amidated C-terminal; ND, not determined.

**Table 2**
Sequence of the signal and prepro regions of the precursor of RegIIA and related A-superfamily α-conotoxins precursors. Alignment was performed using Clustal 2.1 by means of local pairwise alignment information [50].

| Precursor to | Signal sequence | Prepro region | Ref. |
|---|---|---|---|
| RegIIA | MGMRMMFTVFLLVVLTTTVVSS**T**S- | VRASDGRNAAADN**R**ASDLIAQIV**RR**- | |
| Mr1.1 | MGMRMMFTVF-LVVLATTVVF**T**SD- | -RASDGRKAAAKDKASDLVALTV**K**-- | [31] |
| MII | MGMRMMFTVFLLVVLATTVV**S**FPS- | DRASDGRNAAANDKASDVITLAL**K**-- | [19] |
| Vc1.1 | MGMRMMFTVFLLVVLATTVVS**S**TSG- | RREFRGRNAAAK--ASDLVSLTD**KKR** | [37] |
| PnIA | MGMRMMFTVFLLVVLATTVVSF**T**S- | DRASDDGNAAAS----DLIALTI**K**-- | [60] |
| LtIA | MGMRMMFIMFMLVVLATTVV**T**FTS- | DRALDAMNAAASNKASRLIALAV**R**-- | [54] |

Dashes denote gaps. Amino acid conservations are denoted by light grey shade segments and an asterisk (*), whereas colons (:) and periods (.) represent a high and low degree of similarity respectively. Dark grey shaded amino acids are homologous within loci of the set. Bold-faced amino acids are points of cleavage for the release of the signal peptide or the mature α-conotoxin. See Table 1 for the sequences of corresponding mature α-conotoxins.

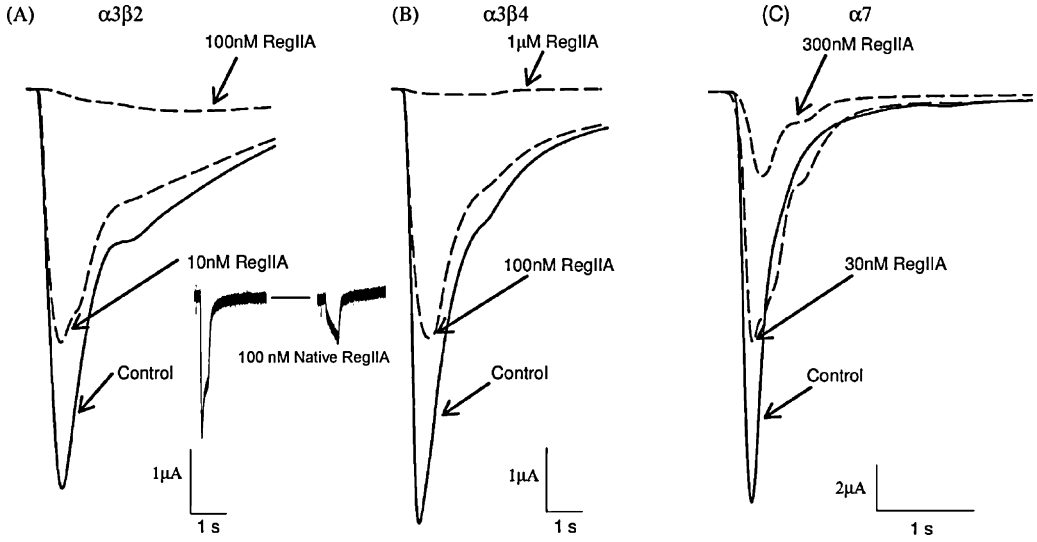


**Fig. 2.** Concentration-dependent inhibition of ACh-evoked current amplitude by RegIIA (synthetic). Representative superimposed ACh-evoked currents recorded in the absence and presence of RegIIA at α3β2 (A), α3β4 (≡), and α7 (C) nAChR subunits expressed in *Xenopus* oocytes. Inset in (A) are current responses of *Xenopus* oocytes expressing α3β2 nAChRs to 70 μM ACh before and after 5 min incubation with 100 nM native RegIIA (scale: $y$ = 100 nA, $x$ = 20 s).

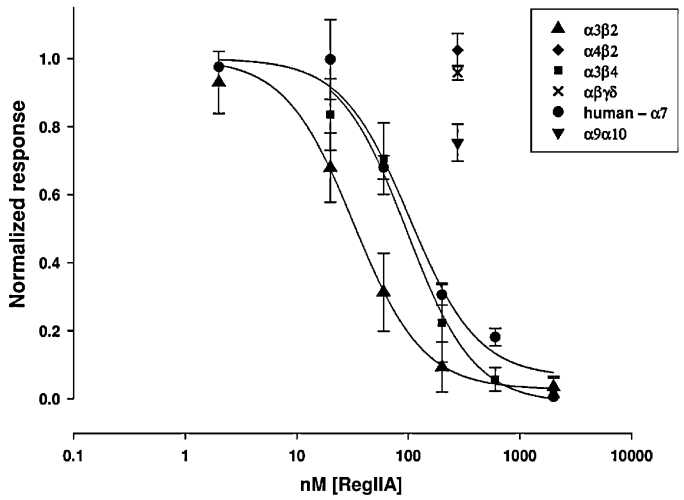


**Fig. 3.** Selectivity of RegIIA inhibition of nAChR subtypes. 1 μM RegIIA completely inhibited α3β2, α3β4 and human α7 receptors and inhibited α9α10 receptors by 22%. Concentration–response curves obtained for RegIIA inhibition gave $IC_{50}$'s of 33 nM for α3β2 (▲; $n$ = 5–8), 97 nM for α3β4 (■; $n$ = 5) and 103 nM for human α7 (●; $n$ = 5–8).

Val-10, and Ile-15, were readily identified in the 2D-TOCSY, thus facilitating the sequence-specific assignment process. Several $HN_i$ to $HN_{i+1}$ correlations along with $\alpha H_i$ to $HN_{i+1}$ in the fingerprint region of the 2D-NOESY completed the assignments.

The secondary shift plot [22] of RegIIA (Fig. 4A) has negative values for the $Pro^6$ to $Val^{10}$ segment, indicative of a helical structure. A comparison of the secondary shifts with Vc1.1 [23] and MII [24] indicate similar folds for all three peptides.

### 3.5. 3D structure of RegIIA

The three-dimensional structures of RegIIA were calculated with 60 NOE-derived distance restraints and 19 dihedral-derived constraints. A set of 50 structures was calculated using CNS [25] and the 20 lowest energy structures chosen to represent the structure of RegIIA. These structures were overlaid over residues $Cys^3$-$Pro^{13}$, as the N- and C-terminal ends are more disordered, with a backbone RMSD of 0.6 ± 0.2 Å (Fig. 4B). A Promotif evaluation of the lowest energy structures indicated that the major element of secondary structure is a helix between residues 6–9 consistent with the chemical shift analysis. The overall fold of RegIIA is highly compact; the location of the disulfide bonds keeps the structure together in a way that the N and C termini are restricted to close

**Table 3**
$IC_{50}$ values (nM) of RegIIA ($n \geq 5$) and related α-conotoxins for nAChR subtypes.

| nAChR/α-conotoxin | α3β4 | α3β2 | α7 | α4β2 | α9α10 | Ref. |
|---|---|---|---|---|---|---|
| RegIIA | 97 ± 20 | 33 ± 4 | 103 ± 23 | >1000 | >1000 | This work |
| OmIA | >10,000 | 11 | 27 | >10,000 | ND | [28] |
| GIC | 755 | 1.1 | ND | 309 | ND | [29] |
| PeIA | 480 | 23 | 1800 | >10,000 | 6.9 | [45] |
| AnIB | ~1000 | 0.3 | 76 | ~1000 | ND | [32] |
| GID | >10,000 | 3.1 | 4.5 | 152 | ND | [30] |
| MII | >1000 | 0.5 | ~200 | >1000 | >1000 | [14] |
| PIA | 518 | 74.2 | ND | >10,000 | ND | [41] |
| Vc1.1 | 4200 | 7300 | >30,000 | >30,000 | 109 | [45] |
| AuIB | 770 | >10,000 | >10,000 | >10,000 | >1000 | [39] |
| PnIA | >1000 | 9.6 | 252 | >1000 | ND | [34] |

ND, not determined.

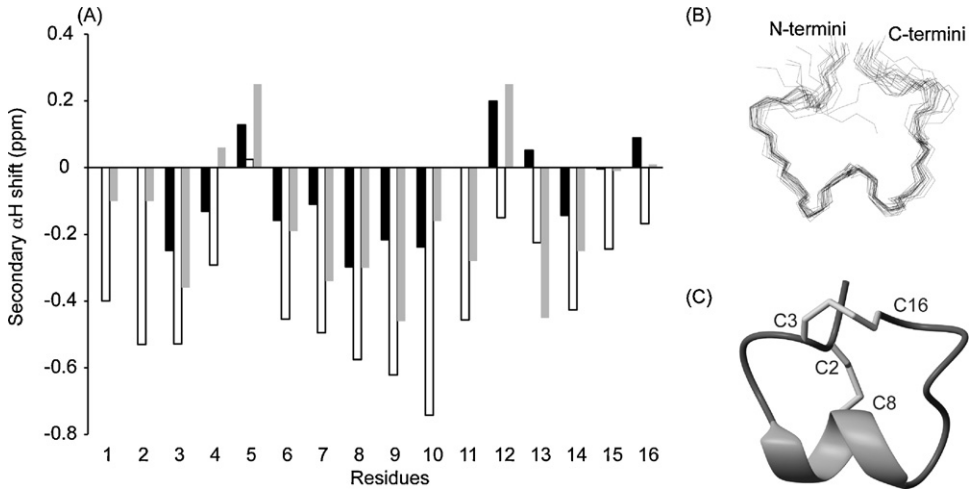


**Fig. 4.** Structure determination of RegIIA. (A) Secondary shift analysis of RegIIA (black bars), Vc1.1 (white bars) and MII (grey bars). (B) Overlay of the 20-lowest energy structures of RegIIA. (C) Ribbon representation of the lowest energy structure of RegIIA with the helical structure shown as a thickened ribbon and the disulfide bonds shown in stick format.

proximity, whereas the $Cys^3$–$Cys^8$ bridge forces the middle of the main chain into close proximity with the C-terminus. The rigidity of the system is completed with $Cys^2$–$Cys^{16}$, which keeps the compactness of the scaffold. The compact fold of the structure forced the main chain into several turns to fit the covalent structure requirements imposed by the disulfide bridges.

Fig. 5 shows an overlay of the average structures of RegIIA and OmIA [26]. There are striking similarities between the NMR structures of these two conotoxins. It is apparent from this comparison that these two conotoxins share the same fold of the main chain of most α-conotoxins, along with the covalent Cys framework. Therefore, the distribution of charged, polar, and hydrophobic residues in the surface of RegIIA may account for their differences in selectivity. Two views of the electrostatic surfaces of RegIIA are given in Fig. 5, highlighting the different faces of the molecule.

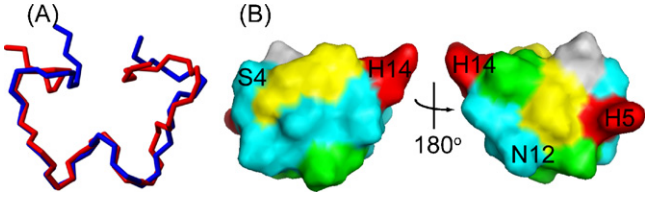


**Fig. 5.** Structure of RegIIA. (A) comparison of RegIIA (red) and OmIA (blue; PDB code 2GCZ). (B) Surface representation of the lowest energy structure of RegIIA. Cystine residues are shown yellow, histidine in red, hydrophobic in green and polar residues in cyan.

## 4. Discussion

Here we describe the isolation and characterization of RegIIA, an α4/7-conotoxin from the venom a *C. regius*, a Western Atlantic worm-hunting cone snail species. This conotoxin, initially described as reg2a [27], has a sequence remarkably similar to OmIA [28], an α-conotoxin from *Conus omaria*, an Indo-Pacific mollusk-hunting species. These two conotoxins only differ in presence of an additional Gly residue at the C-terminal in OmIA. RegIIA has also significant sequence homology with GIC [29] and GID [30], which are α-conotoxins isolated from the venom of *Conus geographus*, an Indo-Pacific fish-hunting species. Given the homology to these α-conotoxins, we initially investigated the activity of native RegIIA on α3β2 nAChRs, resulting in an estimated $IC_{50}$ of 50 nM, a common trait among the α-conotoxins shown in Table 1. However, RegIIA is a potent antagonist of the α3β4 nAChR subtype.

RegIIA has a –SHPA– sequence in its first loop, which is shared with a selected group of α-conotoxins (Table 1). In the second loop RegIIA has a –NNP– motif, which is also shared by OmIA, Mr1.1 [31], AnIB [32], GID, EpI [33] and PnIA [34]. This Pro in the second loop is noteworthy, as cis/trans isomerism at this residue may play a role in the overall conformation of these peptides.

The sequence of the precursor of RegIIA contains a signal sequence that unequivocally places it in the A-superfamily of conotoxins. This signal sequence is essentially identical to other α-conotoxin precursors (Table 2). However, the prepro region of RegIIA shows sequence divergence among the panel of conotoxin precursors shown in Table 2. The prepro region has been

implicated in the secretory pathway of hydrophobic O-superfamily conotoxins [35]; however, its role in the folding and the posttranslational processing within the A-superfamily of conotoxins has not been studied extensively [36]. Other α-conotoxins isolated from *C. regius* show hydroxylation at the conserved Pro in loop one [27], a rare finding among A-superfamily conotoxins. Likewise, vc1a, the native α-conotoxin found the venom duct of *Conus victoriae* is also hydroxylated at that Pro [37]. Given that the most sequence divergence among these conotoxin precursors is at the prepro region, it is likely that this segment of the precursor is implicated in posttranslational processing. The prepro region binds to protein disulfide isomerase (PDI), which is a subunit of prolyl 4-hydroxylase (P4H), the enzyme catalyzing hydroxylation of proline residues [36]. The involvement of other proteins in the *in vivo* oxidative folding pathway of conotoxins precursors, such as PPI, can be expected [38]. In all these events, the prepro region appears to have a central role in directing the final conformation and level of modification of the mature toxin.

The ability of RegIIA to block α3β4 nAChRs at low nanomolar levels sets it apart from other α4/7-conotoxins. Weak inhibition of α3β4 is observed for AuIB [39], PeIA [40], GIC [29] and PIA [41] (Table 3). BuIA, an unusual α4/4-conotoxin discovered from the venom of *Conus bullatus*, also shows potent inhibition of α3β4 nAChRs [42]. With the exception of AuIB, these conotoxins inhibit other nAChR subtypes more potently. Despite its weak inhibition of α3β4 nAChRs, AuIB appears to be selective; however, it has been found that this α-conotoxin potently activates $GABA_BR$, and has been shown to produce analgesia by inhibiting $Ca_V2.2$ channels [43]. PeIA [44], Vc1.1 [45] and Vc1.2 [46] also share this trait, but not RegIIA (Table 1), which exhibited no effect on this $GABA_BR$ mediated pathway (data not shown).

The selectivity profiles of α-conotoxins are known to change with single amino acid replacements [13,47–50]. This is the case with RegIIA, as its sequence differs only by one amino acid with OmIA, and three for PeIA. These differences translate into marked differences in their selectivity profiles. In addition to the unusual low nanomolar α3β4 inhibition by RegIIA, this conotoxin can block α7 nAChRs, whereas PeIA does not. Conversely, PeIA potently inhibits α9α10 nAChRs and modulates $Ca_V2.2$ via $GABA_BR$, whereas RegIIA does not. Several scenarios can be envisioned to explain these changes in selectivity profiles with subtle differences in α-conotoxin sequences. These differences can have profound implications in the recognition of α-conotoxins by the receptor binding site. The delicate complementary shapes of the ligand and receptor can be easily upset by the presence of an additional amino acid or the lack of appropriate interactions between ligand and receptor, whether this occurs by fitting of the native structure of the ligand or receptor-induced conformation of the ligand to induce binding. The structures of α-conotoxins bound to AChBPs suggest the former as a more likely scenario [51]. However, there are some differences between the AChBP-bound structure of α-conotoxins and their unbound counterparts [52]. Furthermore, α-conotoxins such as ImI can bind to nAChRs in their desensitized conformation, whereas others, such as PnIA, bind to nAChRs in their resting state [52]. All these considerations can contribute to the complex and delicate scenario that plays into the selectivity profiles of α-conotoxins towards nAChRs.

Conotoxin interactions with nAChRs can be further complicated by the existence of multiple microsites for conotoxins binding, i.e., α-conotoxins ImI and ImII bind to different microsites of α7 nAChRs, a switch that is caused by a three amino acid difference in the sequence of these related peptides [53]. Some nAChRs present a more complicated scenario, as multiple microsites for α-conotoxin binding to α3β2 and α3β4 nAChRs have been proposed and rationalized using molecular models [54,55]. Further experiments on the binding of RegIIA to these nAChRs and their analogs will be necessary to assess the precise binding mode of this peptide.

RegIIA is among the most potent inhibitor of α3β4 nAChRs to date. This is of particular significance, as it does not inhibit the α4β2 subtype (Table 3). This feature makes RegIIA a suitable probe to evaluate nicotine addiction processes. It has been shown that α4β2 nAChRs are required for nicotine addition and dependence [3], therefore, these receptors are actively pursued as targets for tobacco smoking cessation therapeutics [56]. However, other nAChR subtypes are also implicated in addiction to nicotine and other drugs of abuse. Particularly, antagonism of α3β4 nAChRs has been proposed as a strategy to reduce self-administration of opiates and other stimulants [57]. The involvement of α3β4 receptors in nicotine addiction processes has been demonstrated by a reduced nicotine-induced hypolocomotion in β4 null mice [5]. However, further exploration of these findings has been hampered by the lack of tools to explore the role of α3β4 nAChRs. The selectivity profile of RegIIA can provide advancement towards this end. However, as is the case for other related α-conotoxins, RegIIA also blocks α7 and α3β2 nAChRs (Table 3). While structurally related to other α-conotoxins, RegIIA has an exquisite balance of shape, charges, and polarity exposed on its structure to potently block the α3β4 nAChR subtype. Improving the selectivity of RegIIA towards α3β4 nAChRs can be achieved by judicious design of RegIIA analogs (currently in progress). These studies can be valuable tools for further exploring ligand–receptor interactions and in the design of novel α-conotoxins with improved selectivity.

In summary, we have discovered an α-conotoxin with a unique selectivity profile, which includes low nanomolar blockage of α3β4 nAChRs. This feature may lead to a better understanding of structural features for selectivity and function of nAChRs. Such selective profiles and potent blockage of α3β4 nAChRs will be useful for testing the hypothesis that α3β4 receptor antagonists can attenuate rewarding properties of nicotine and other drugs of abuse [57,58].

## Acknowledgments

This research was supported by the National Institutes of Health (NIH) Grants 1R15GM066004-01A1 and 1R21NS066371-01 (FM); The Florida Seagrant program Grant R/LR-MB-28 (FM); Australian Research Council Discovery Project Grant (DJA, DJC and FM); Australian Research Council Professorial Fellowship (DJA); Australian National Health and Medical Research Grant (PFA and KBA); "LOEWE–Landes-Offensive zur Entwicklung Wissenschaftlich-ökonomischer Exzellenz" of Hesse's Ministry of Higher Education, Research, and the Arts (CM).

## References

[1] Albuquerque EX, Pereira EF, Alkondon M, Rogers SW. Mammalian nicotinic acetylcholine receptors: from structure to function. Physiol Rev 2009;89:73–120.
[2] Millar NS, Gotti C. Diversity of vertebrate nicotinic acetylcholine receptors. Neuropharmacology 2009;56:237–46.
[3] Rose JE. Multiple brain pathways and receptors underlying tobacco addiction. Biochem Pharmacol 2007;74:1263–70.
[4] Tapper AR, McKinney SL, Nashmi R, Schwarz J, Deshpande P, Labarca C, et al. Nicotine activation of α4* receptors: sufficient for reward, tolerance, and sensitization. Science 2004;306:1029–32.
[5] Salas R, Cook KD, Bassetto L, De Biasi M. The α3 and β4 nicotinic acetylcholine receptor subunits are necessary for nicotine-induced seizures and hypolocomotion in mice. Neuropharmacology 2004;47:401–7.
[6] Improgo MR, Scofield MD, Tapper AR, Gardner PD. The nicotinic acetylcholine receptor CHRNA5/A3/B4 gene cluster: dual role in nicotine addiction and lung cancer. Prog Neurobiol 2010;92:212–26.
[7] Azam L, McIntosh JM. α-Conotoxins as pharmacological probes of nicotinic acetylcholine receptors. Acta Pharmacol Sin 2009;30:771–83.
[8] Yen TY, Yan H, Macher BA. Characterizing closely spaced, complex disulfide bond patterns in peptides and proteins by liquid chromatography/electrospray ionization tandem mass spectrometry. J Mass Spectrom 2002;37:15–30.

[9] Kauferstein S, Melaun C, Mebs D. Direct cDNA cloning of novel conopeptide precursors of the O-superfamily. Peptides (New York NY United States) 2005;26:361–7.
[10] Wang C-Z, Jiang H, Ou Z-L, Chen J-S, Chi C-W. cDNA cloning of two A-superfamily conotoxins from *Conus striatus*. Toxicon 2003;42:613–9.
[11] Tamura K, Dudley J, Nei M, Kumar S. MEGA4: Molecular Evolutionary Genetics Analysis (MEGA) software version 4.0. Mol Biol Evol 2007;24:1596–9.
[12] Schnolzer M, Alewood P, Jones A, Alewood D, Kent SB. In situ neutralization in Boc-chemistry solid phase peptide synthesis Rapid, high yield assembly of difficult sequences. Int J Pept Protein Res 1992;40:180–93.
[13] Hogg RC, Hopping G, Alewood PF, Adams DJ, Bertrand D. α-Conotoxins PnIA and [A10L]PnIA stabilize different states of the α7-L247T nicotinic acetylcholine receptor. J Biol Chem 2003;278:26908–14.
[14] Everhart D, Cartier GE, Malhotra A, Gomes AV, McIntosh JM, Luetje CW. Determinants of potency on α-conotoxin MII, a peptide antagonist of neuronal nicotinic receptors. Biochemistry 2004;43:2732–7.
[15] Nevin ST, Clark RJ, Klimis H, Christie MJ, Craik DJ, Adams DJ. Are α9α10 nicotinic acetylcholine receptors a pain target for α-conotoxins? Mol Pharmacol 2007;72:1406–10.
[16] Pisarewicz K, Mora D, Pflueger FC, Fields GB, Mari F. Polypeptide chains containing D-γ-hydroxyvaline. J Am Chem Soc 2005;127:6207–15.
[17] Millard EL, Nevin ST, Loughnan ML, Nicke A, Clark RJ, Alewood PF, et al. Inhibition of neuronal nicotinic acetylcholine receptor subtypes by α-conotoxin GID and analogues. J Biol Chem 2009;284:4944–51.
[18] Altschul SF, Madden TL, Schaffer AA, Zhang JH, Zhang Z, Miller W, et al. Gapped BLAST and PSI-BLAST: a new generation of protein database search programs. Nucleic Acids Res 1997;25:3389–402.
[19] Santos AD, McIntosh JM, Hillyard DR, Cruz LJ, Olivera BM. The A-superfamily of conotoxins: structural and functional divergence. J Biol Chem 2004;279:17596–606.
[20] Corpuz GP, Jacobsen RB, Jimenez EC, Watkins M, Walker C, Colledge C, et al. Definition of the M-conotoxin superfamily: characterization of novel peptides from molluscivorous conus venoms. Biochemistry 2005;44:8176–86.
[21] Wuthrich K. NMR of Proteins and Nucleic Acids. New York: Wiley; 1986.
[22] Wishart DS, Sykes BD, Richards FM. The chemical shift index: a fast and simple method for the assignment of protein secondary structure through NMR spectroscopy. Biochemistry 1992;31:1647–51.
[23] Clark RJ, Fischer H, Nevin ST, Adams DJ, Craik DJ. The synthesis, structural characterization, and receptor specificity of the α-conotoxin Vc1.1. J Biol Chem 2006;281:23254–63.
[24] Hill JM, Oomen CJ, Miranda LP, Bingham J-P, Alewood PF, Craik DJ. Three-dimensional solution structure of α-conotoxin MII by NMR spectroscopy: effects of solution environment on helicity. Biochemistry 1998;37:15621–30.
[25] Brunger AT. Version 1.2 of the Crystallography and NMR system. Nat Protoc 2007;2:2728–33.
[26] Chi S-W, Kim D-H, Olivera BM, McIntosh JM, Han K-H. Solution conformation of a neuronal nicotinic acetylcholine receptor antagonist α-conotoxin OmIA that discriminates α3 vs α6 nAChR subtypes. Biochem Biophys Res Commun 2006;345:248–54.
[27] Franco A, Pisarewicz K, Moller C, Mora D, Fields GB, Mari F. Hyperhydroxylation: a new strategy for neuronal targeting by venomous marine molluscs. Prog Mol Subcell Biol 2006;43:83–103.
[28] Talley TT, Olivera BM, Han K-H, Christensen SB, Dowell C, Tsigelny I, et al. α-Conotoxin OmIA Is a potent ligand for the acetylcholine-binding protein as well as α3β2 and α7 nicotinic acetylcholine receptors. J Biol Chem 2006;281:24678–86.
[29] McIntosh JM, Dowell C, Watkins M, Garrett JE, Yoshikami D, Olivera BM. α-Conotoxin GIC from *Conus geographus*, a novel peptide antagonist of nicotinic acetylcholine receptors. J Biol Chem 2002;277:33610–5.
[30] Nicke A, Loughnan ML, Millard EL, Alewood PF, Adams DJ, Daly NL, et al. Isolation, structure, and activity of GID, a novel α4/7-conotoxin with an extended N-terminal sequence. J Biol Chem 2003;278:3137–44.
[31] Peng C, Chen W, Sanders T, Chew G, Liu J, Hawrot E, et al. Chemical synthesis and characterization of two α4/7-conotoxins. Acta Biochim Biophys Sin (Shanghai) 2010;42:745–53.
[32] Loughnan ML, Nicke A, Jones A, Adams DJ, Alewood PF, Lewis RJ. Chemical and functional identification and characterization of novel sulfated α-conotoxins from the cone snail *Conus anemone*. J Med Chem 2004;47:1234–41.
[33] Loughnan M, Bond T, Atkins A, Cuevas J, Adams DJ, Broxton NM, et al. α-Conotoxin EpI, a novel sulfated peptide from *Conus episcopatus* that selectively targets neuronal nicotinic acetylcholine receptors. J Biol Chem 1998;273:15667–74.
[34] Fainzilber M, Hasson A, Oren R, Burlingame AL, Gordon D, Spira ME, et al. New mollusk-specific α-conotoxins block aplysia neuronal acetylcholine receptors. Biochemistry 1994;33:9523–9.
[35] Conticello SG, Kowalsman ND, Jacobsen C, Yudkovsky G, Sato K, Elazar Z, et al. The prodomain of a secreted hydrophobic mini-protein facilitates its export from the endoplasmic reticulum by hitchhiking on sorting receptors. J Biol Chem 2003;278:26311–4.
[36] Buczek O, Olivera BM, Bulaj G. Propeptide does not act as an intramolecular chaperone but facilitates protein disulfide isomerase-assisted folding of a conotoxin precursor. Biochemistry 2004;43:1093–101.
[37] Jakubowski JA, Keays DA, Kelley WP, Sandall DW, Bingham J-P, Livett BG, et al. Determining sequences and post-translational modifications of novel conotoxins in *Conus victoriae* using cDNA sequencing and mass spectrometry. J Mass Spectrom 2004;39:548–57.
[38] Safavi-Hemami H, Bulaj G, Olivera BM, Williamson NA, Purcell AW. Identification of Conus peptidylprolyl cis-trans isomerases (PPIases) and assessment of their role in the oxidative folding of conotoxins. J Biol Chem 2010;285:12735–46.
[39] Luo S, Kulak JM, Cartier GE, Jacobsen RB, Yoshikami D, Olivera BM, et al. α-Conotoxin AuIB selectively blocks α3β4 nicotinic acetylcholine receptors and nicotine-evoked norepinephrine release. J Neurosci 1998;18:8571–9.
[40] McIntosh JM, Plazas PV, Watkins M, Gomez-Casati ME, Olivera BM, Elgoyhen AB. A novel α-conotoxin, PeIA, cloned from *Conus pergrandis*, discriminates between rat α9α10 and α7 nicotinic cholinergic receptors. J Biol Chem 2005;280:30107–12.
[41] Dowell C, Olivera BM, Garrett JE, Staheli ST, Watkins M, Kuryatov A, et al. α-Conotoxin PIA is selective for α6 subunit-containing nicotinic acetylcholine receptors. J Neurosci 2003;23:8445–52.
[42] Azam L, Dowell C, Watkins M, Stitzel JA, Olivera BM, McIntosh JM. α-Conotoxin BuIA, a novel peptide from *Conus bullatus*, distinguishes among neuronal nicotinic acetylcholine receptors. J Biol Chem 2005;280:80–7.
[43] Klimis H, Adams DJ, Callaghan B, Nevin S, Alewood PF, Vaughan CW, et al. A novel mechanism of inhibition of high-voltage activated calcium channels by α-conotoxins contributes to relief of nerve injury-induced neuropathic pain. Pain 2011;152:259–66.
[44] Daly NL, Callaghan B, Clark RJ, Nevin ST, Adams DJ, Craik DJ. Structure and activity of α-conotoxin PeIA at nicotinic acetylcholine receptor subtypes and $GABA_B$ receptor-coupled N-type calcium channels. J Biol Chem 2011;286:10233–7.
[45] Callaghan B, Haythornthwaite A, Berecki G, Clark RJ, Craik DJ, Adams DJ. Analgesic alpha-conotoxins Vc1.1 and Rg1A inhibit N-type calcium channels in rat sensory neurons via $GABA_B$ receptor activation. J Neurosci 2008;28:10943–51.
[46] Safavi-Hemami H, Siero WA, Kuang Z, Williamson NA, Karas JA, Page LR, et al. Embryonic toxin expression in the cone snail *Conus victoriae*—primed to kill or divergent function? J Biol Chem 2011;286:22546–57.
[47] Dai Q, Castellino FJ, Prorok M. A single amino acid replacement results in the $Ca^{2+}$-induced self-assembly of a helical conantokin-based peptide. Biochemistry 2004;43:13225–32.
[48] Jacobsen RB, Koch ED, Lange-Malecki B, Stocker M, Verhey J, Van Wagoner RM, et al. Single amino acid substitutions in κ-conotoxin PVIIA disrupt interaction with the Shaker $K^+$ channel. J Biol Chem 2000;275:24639–44.
[49] Hogg RC, Miranda LP, Craik DJ, Lewis RJ, Alewood PF, Adams DJ. Single amino acid substitutions in α-conotoxin PnIA shift selectivity for subtypes of the mammalian neuronal nicotinic acetylcholine receptor. J Biol Chem 1999;274:36559–64.
[50] Teichert RW, Lopez-Vera E, Gulyas J, Watkins M, Rivier J, Olivera BM. Definition and characterization of the short αA-conotoxins: a single residue determines dissociation kinetics from the fetal muscle nicotinic acetylcholine receptor. Biochemistry 2006;45:1304–12.
[51] Celie PH, Kasheverov IE, Mordvintsev DY, Hogg RC, van Nierop P, van Elk R, et al. Crystal structure of nicotinic acetylcholine receptor homolog AChBP in complex with an α-conotoxin PnIA variant. Nat Struct Mol Biol 2005;12:582–8.
[52] Ulens C, Hogg RC, Celie PH, Bertrand D, Tsetlin V, Smit AB, et al. Structural determinants of selective α-conotoxin binding to a nicotinic acetylcholine receptor homolog AChBP. Proc Natl Acad Sci USA 2006;103:3615–20.
[53] Ellison M, McIntosh JM, Olivera BM. α-Conotoxins ImI and ImII similar α7 nicotinic receptor antagonists act at different sites. J Biol Chem 2003;278:757–64.
[54] Luo S, Akondi KB, Zhangsun D, Wu Y, Zhu X, Hu Y, et al. Atypical α-conotoxin LtIA from *Conus litteratus* targets a novel microsite of the α3β2 nicotinic receptor. J Biol Chem 2010;285:12355–66.
[55] Grishin AA, Wang CI, Muttenthaler M, Alewood PF, Lewis RJ, Adams DJ. α-conotoxin AuIB isomers exhibit distinct inhibitory mechanisms and differential sensitivity to stoichiometry of α3β4 nicotinic acetylcholine receptors. J Biol Chem 2010;285:22254–63.
[56] Jorenby DE, Hays JT, Rigotti NA, Azoulay S, Watsky EJ, Williams KE, et al. Efficacy of varenicline, an α4β2 nicotinic acetylcholine receptor partial agonist, vs placebo or sustained-release bupropion for smoking cessation: a randomized controlled trial. JAMA 2006;296:56–63.
[57] Glick SD, Maisonneuve IM, Kitchen BA, Fleck MW. Antagonism of α3β4 nicotinic receptors as a strategy to reduce opioid and stimulant self-administration. Eur J Pharmacol 2002;438:99–105.
[58] Zaveri N, Jiang F, Olsen C, Polgar W, Toll L. Novel α3β4 nicotinic acetylcholine receptor-selective ligands. Discovery, structure-activity studies, and pharmacological evaluation. J Med Chem 2010;53:8187–91.
[59] Larkin MA, Blackshields G, Brown NP, Chenna R, McGettigan PA, McWilliam H, et al. Clustal W and Clustal X version 2.0. Bioinformatics 2007;23:2947–8.
[60] Conticello SG, Gilad Y, Avidan N, Ben-Asher E, Levy Z, Fainzilber M. Mechanisms for evolving hypervariability: the case of conopeptides. Mol Biol Evol 2001;18:120–31.